

Determination of Higgs-boson couplings (SFitter)

Michael Rauch*

Institut für Theoretische Physik, Karlsruher Institut für Technologie (KIT), Karlsruhe, Germany

DOI: will be assigned

After the discovery of a Higgs boson, the next step is to measure its properties and test their accordance with the predictions of the Standard Model, in particular the couplings of the Higgs boson. In this talk we discuss what information the LHC will be able to give us over the coming years, and what remains as a task for a future Linear Collider.

Using the well-established SFitter framework, we map measurements onto a weak-scale effective theory with general Higgs boson couplings. Our sophisticated error treatment allows us to take all theory and experimental errors, including arbitrary correlations, fully into account.

1 Introduction

Completing our understanding of the electro-weak symmetry-breaking mechanism is one of the main tasks for present and future particle colliders. In the Standard Model (SM), this is accomplished by introducing a complex $SU(2)$ doublet, the Higgs field, which obtains a vacuum expectation value (vev) [1, 2, 3]. Three of the four degrees of freedom form the longitudinal modes of W and Z bosons, while the remaining one becomes a physical particle, the Higgs boson. Interactions between these gauge bosons and the Higgs field are introduced automatically via the latter's kinetic term, while interactions with fermions are added via Yukawa-type couplings. Replacing the Higgs field by its vev then yields mass terms for the gauge bosons and fermions. Therefore, the couplings of the Higgs boson to the other particles are fixed and proportional to the measured masses and the vev.

The mass of the Higgs boson is the only remaining unknown parameter in the SM. Direct searches by LEP [4], Tevatron [5] and in particular the LHC experiments ATLAS [6] and CMS [7] have excluded large parts of the parameter space, leaving only a small window around 125 GeV. High-mass values, where the experimental sensitivity drops again, are strongly disfavoured by indirect constraints from electro-weak precision data [8, 9]. As mentioned before, the Higgs couplings in the SM are completely determined by the known particle masses. Therefore, we can use these theoretically predicted values and compare them to future measurements of Higgs boson channels [10, 11, 12, 13, 14, 15, 16]. Thereby, we assume that the discrete quantum numbers, like its CP property or spin [17], are identical to the SM expectation. Many models of new physics predict deviations in the Higgs couplings, which can then be measured. Examples include models with an extended Higgs sector, like the two-Higgs doublet structure e.g. in supersymmetry [18], or also Higgs portal models [19], but modifications can also be more elementary as in composite models [20], where the Higgs boson emerges as a pseudo-Goldstone boson of a new strongly-interacting sector.

A correct treatment of all errors is important to obtain correct results. As in the Higgs boson channels rates are measured, these statistical errors are of the Poisson type. Additionally, there are systematic errors, which are correlated, and we implement the full correlation matrix between different measurements. Theory errors are best described as box-shaped [3], using the prescription of the RFit scheme [21]. In the SFitter tool [22] these different types of errors are fully implemented. As output we obtain a fully-dimensional log-likelihood map, which we can then reduce to plotable one- or two-dimensional distributions via both Bayesian (marginalisation) and Frequentist (profile likelihood) techniques. Furthermore, a list of best-fitting points is obtained.

*for the SFitter collaboration

2 Setup of the Calculation

As the underlying model of our study we assume the Standard Model with a generalised Higgs sector, where the Higgs couplings can take arbitrary values. These are parametrised in the following way: Couplings to particles i , which are present at tree-level in the SM, are modified according to

$$g_{iH} \rightarrow g_{iH}^{\text{SM}}(1 + \Delta_{iH}) . \quad (1)$$

As a global sign flip of all couplings is not observable, we always take g_{WWH} to be positive, *i.e.* $\Delta_{WWH} > -1$. Additionally, there are two important loop-induced couplings present, namely those to gluons and photons. They are altered in the following way:

$$g_{iH} \rightarrow g_{iH}^{\text{SM}}(1 + \Delta_{iH}^{\text{SM}} + \Delta_{iH}) . \quad (2)$$

These can receive two types of contributions. First, there are contributions from changing the tree-level couplings, Δ_{iH}^{SM} . Second, there can be additional dimension-five contributions Δ_{iH} . They originate from new particles running in the loop, e.g. the supersymmetric partners in SUSY models. The numerical values of the couplings are obtained from a modified version of HDecay [23]. Also the masses of the Higgs boson and the top and bottom quark are added as free parameters and corresponding measurements constrain them to their experimentally measured value. Additionally, we define Δ_H as a single free parameter that changes all (tree-level) couplings simultaneously.

The total width of the Higgs boson is too small to be measured directly at the LHC. Therefore we have to make one single model assumption about how to treat the total width, which we take as

$$\Gamma_{\text{tot}} = \sum_{\text{obs}} \Gamma_i(g_{iH}) + \text{generation universality} .$$

This means that there are no further contributions from Higgs decays into invisible particles. The assumption about generation universality is important as the Higgs has a significant branching ratio of several percent into unobservable particles (e.g. charm quarks) for which at the LHC there is no possibility to measure them, and neglecting them would introduce a bias. Further details of the setup have been described in Refs. [11, 12]. We will not consider any couplings that can only be measured with very high luminosity or not at all. This includes the only second-generation Yukawa coupling that might be measurable at the LHC, namely those to muons [24, 25], as well as the Higgs self-couplings [26, 27, 28, 29].

3 Results

3.1 Expectations for the LHC at 14 TeV

The measurements that enter our analysis are derived from an ATLAS Monte Carlo study performed for an integrated luminosity of 30 fb^{-1} and assuming a centre-of-mass energy of 14 TeV [11, 30]. We perform a simulation with typically 5000 toy Monte Carlos, where we smear the signal and background expectations according to their corresponding errors, and fit the resulting Higgs couplings.

In Fig. 1 we show the results of our analysis. The different curves denote the 68% CL errors on the Δ_{iH} parameter for the respective coupling. As input value for the signal strength we assume a SM Higgs boson of the given mass value and note that for reduced couplings the change in the absolute value of the errors is small. On the left-hand side of the figure we present results where additional contributions from dimension-five operators have been neglected. Also shown is the result for the single-parameter modifier Δ_H . On the right-hand side the dimension-five operators are taken into account as well. In both cases the coupling of the Higgs to W bosons can be measured best, between 10 and 20% over the whole mass range. The dimension-five operators thereby reduce the sensitivity to this coupling somewhat. Yukawa couplings to bottom quarks and τ leptons can only be determined with good accuracy for Higgs masses below 140 to 150 GeV, as for larger masses the corresponding branching ratios become too small. The top quark is strongly affected by the dimension-five operators. Without these operators the gluon-fusion production processes contribute to the precision of this coupling. Including them, the top-quark coupling needs to be determined by the badly measurable top-quark-associated production modes, and gluon-fusion production then pins down the size of the additional operators relative to the top quark coupling.

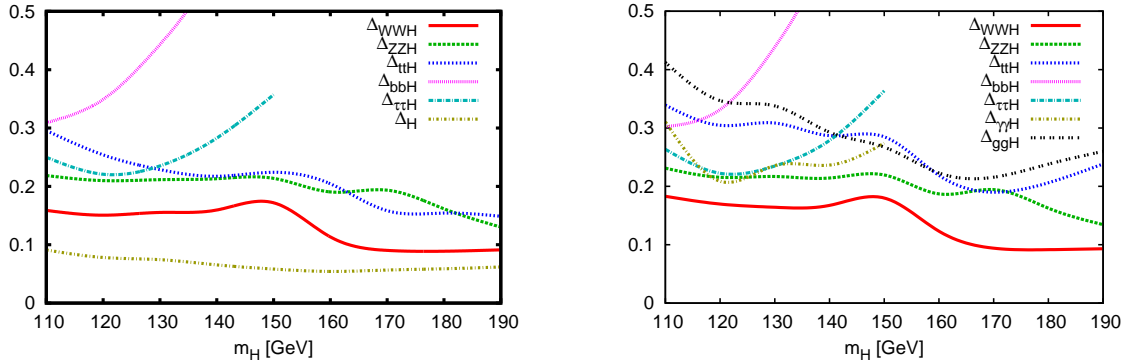


Figure 1: Error on the Higgs-boson couplings as a function of the Higgs mass without (*left*) and including (*right*) additional dimension-five operators. The left-hand plot also includes the result for a single-parameter modification Δ_H . Results are for the LHC at 14 TeV centre-of-mass energy and an integrated luminosity of 30 fb^{-1} , assuming SM Higgs couplings. Figures taken from Ref. [31].

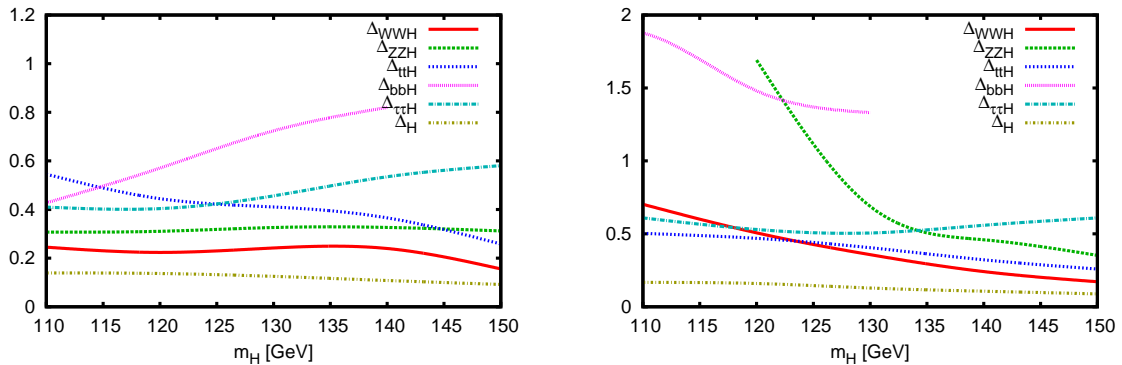


Figure 2: Error on the Higgs-boson couplings as a function of the Higgs mass including (*left*) and without (*right*) the subjet analyses in the Higgsstrahlung production processes with decays into bottom quarks. Results are for the LHC at 7 TeV centre-of-mass energy and an integrated luminosity of 20 fb^{-1} , assuming SM Higgs couplings, obtained by extrapolating the 14-TeV-Monte-Carlo studies.

3.2 Extrapolation to 7 TeV

To get an estimate of what to expect from the LHC in the near future, we have extrapolated these studies to a centre-of-mass energy of 7 TeV. For the backgrounds the inclusive cross sections of the individual contributions were computed with Sherpa [32] and the event rate scaled according to the numbers obtained. For the signal we assume that the signal efficiencies, i.e. the number of signal events remaining after the selection cuts and detector acceptance corrections relative to the original rate, stays unchanged. The cross sections themselves for both centre-of-mass energies are taken from Ref. [3]. As the expected precision on the couplings will be rather low, only the case of vanishing additional dimension-five operators is considered here.

In Fig. 2 we show the corresponding results for an integrated luminosity of 20 fb^{-1} , corresponding to approximately what is expected for the end of 2012¹. On the left-hand side we include all channels of the 14-TeV analysis. We observe the same principal behaviour as in Fig. 1, but with a significant increase in the expected errors. Nevertheless, with this amount of data a determination of Δ_H with a precision of

¹The increased centre-of-mass energy of 8 TeV for the 2012 run can be approximated by a corresponding increase in the integrated luminosity.

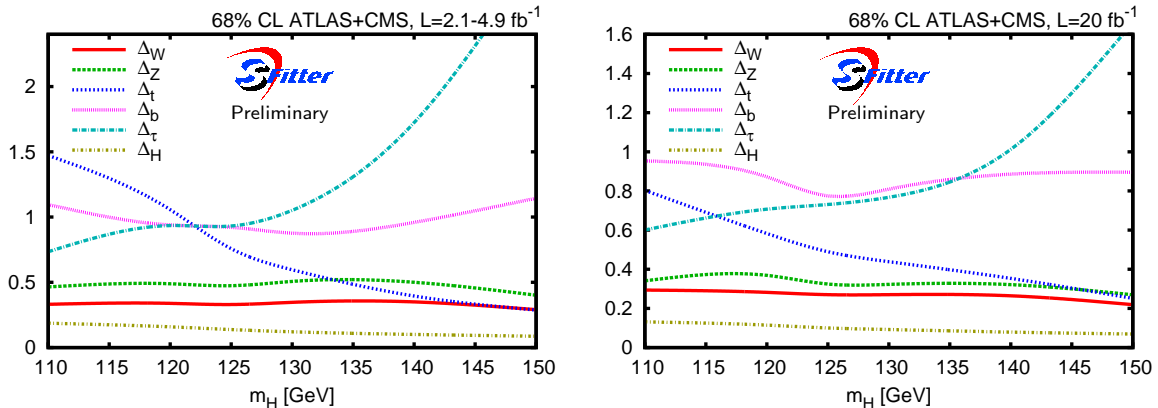


Figure 3: Precision of tree-level Higgs-boson couplings as well as single-parameter modifier as a function of the Higgs mass using current LHC searches as input. Results are presented for the luminosities used in the analyses (*left*) and extrapolated to 20 fb^{-1} (*right*). Figure from Ref. [15].

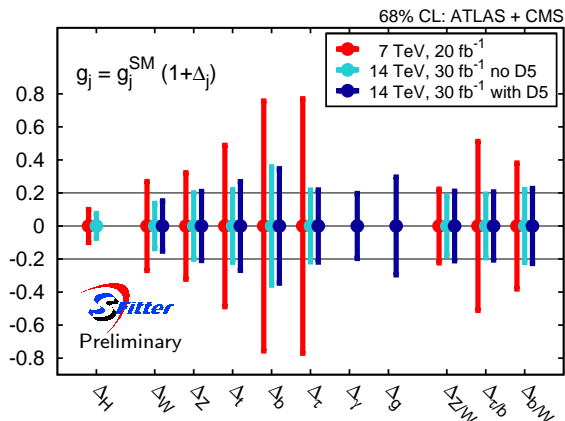


Figure 4: Overview of LHC expectations in different scenarios for energy and integrated luminosity for a SM Higgs boson with mass of 125 GeV. Figure from Ref. [15].

14% is already possible for a Higgs boson mass of 125 GeV. On the right-hand side the channels making use of subjet techniques [33] are removed. These consist of Higgs bosons produced in association with a W or Z boson, where the Higgs decays into bottom quarks and the decay products are required to be strongly boosted in order to reduce backgrounds. A significant drop in accuracy can be observed mainly for two couplings. The coupling to Z bosons is now predominantly determined by the decay of the Higgs to four leptons, which suffers from low event numbers for lighter Higgs masses. The bottom-quark Yukawa coupling has to rely on the top-quark-associated production channel with decays into bottom quarks as well as its contribution to gluon-fusion production. The first one suffers from a large combinatorial background, while in the second case the bottom-quark loop is only a small contribution. The badly determined bottom coupling then influences all other couplings via the total width.

3.3 Results and Expectations from Current Measurements

With direct search results available from the LHC, we can update the results of the previous subsection using the actual background expectations and errors as described in the analyses [6, 7]. Thereby we assume as input that there is a SM Higgs boson at the considered mass value and add a SM Higgs signal to the background expectations. These results are depicted in Fig. 3. On the left we show errors on the Higgs couplings using for each measurement the luminosity for which the analysis has been performed. With this

data a precision of 14% on Δ_H is already possible, and the couplings to the weak bosons can also be measured fairly precisely. The error on the top-quark Yukawa coupling is mostly determined by Higgs production via gluon-fusion decaying into a W pair. The sensitivity of this channel drops rapidly below 125 GeV, leading to the observed behaviour of the top-quark coupling. On the right-hand side we present expectations when extrapolating all analyses to an integrated luminosity of 20 fb^{-1} . This extrapolation is done blindly, i.e. the improvement is purely statistical. The precision on the single-parameter modifier now reaches 9% for a Higgs mass around 125 GeV.

In Fig. 4 the different results shown previously are summarised for a hypothetical Higgs boson at 125 GeV assuming SM couplings as a central value. The three values on the right-hand side of the plot show errors on ratios of couplings. While for the Z over W Higgs couplings at 7 TeV only a small improvement over the absolute measurements is achievable, the situation is different for the two other ratios involving the bottom Yukawa coupling. Here correlations are important and therefore the ratio is better determined. At a 14 TeV LHC the situation is different. Using ratios yields no improvement over absolute values in any case.

4 Models of New Physics

In physics models beyond the Standard Model the couplings between the Higgs boson and the gauge bosons and fermions can be modified from the SM theory prediction. In this section we will discuss two such models, a Higgs portal [19] as well as a strongly-interacting light Higgs [20].

4.1 Higgs Portal

In the Higgs portal model, an additional hidden sector is added which is a singlet under the SM gauge groups. A connection to the SM is only possible via a term connecting the Higgs field of the SM Φ_s with that of the hidden sector Φ_h

$$\mathcal{L} \propto \Phi_s^\dagger \Phi_s \Phi_h^\dagger \Phi_h .$$

After electro-weak symmetry-breaking both fields obtain a vev. The two physical Higgs bosons of the SM and the hidden sector mix and need to be rotated into mass eigenstates

$$\begin{pmatrix} H_1 \\ H_2 \end{pmatrix} = \begin{pmatrix} \cos \chi & \sin \chi \\ -\sin \chi & \cos \chi \end{pmatrix} \begin{pmatrix} H_s \\ H_h \end{pmatrix} . \quad (3)$$

The parameter $\cos \chi$ corresponds to our single-parameter modifier Δ_H defined before. The cross sections and branching ratios then change in the following way from their SM value for H_1

$$\sigma = \cos^2 \chi \cdot \sigma^{\text{SM}} \quad (4)$$

$$\Gamma_{\text{vis}} = \cos^2 \chi \cdot \Gamma_{\text{vis}}^{\text{SM}} \quad (5)$$

$$\Gamma_{\text{inv}} = \cos^2 \chi \cdot \Gamma_{\text{inv}}^{\text{SM}} + \Gamma_{\text{hid}} . \quad (6)$$

$\Gamma_{\text{inv}}^{\text{SM}}$ is induced by Higgs decays into four neutrinos, which has a negligible rate for light Higgs bosons. The partial decay width into the hidden sector Γ_{hid} is a free parameter and depends on the structure, i.e. couplings and masses, of the hidden sector particles, being zero if they are all heavy. Corresponding equations hold for H_2 with the replacement $\cos \chi \leftrightarrow \sin \chi$ plus possibly decays $H_2 \rightarrow H_1 H_1$ added, if this channel is kinematically allowed.

In Fig. 5 we present the fitted $\cos^2 \chi$ as a function of the Higgs mass in a scenario where the Higgs contains no additional decay modes into invisible particles. $\cos^2 \chi$ is a free parameter, which is not constrained to its physical range. On the left-hand side the input value of $\cos^2 \chi$ is chosen as one, corresponding to the SM scenario. Hence, this curve corresponds to the Δ_H line of Fig. 1. The central value is correctly reproduced by the fit. Errors at the 95% CL range between 25% and 50% with the highest precision obtainable for a mass of 170 GeV. On the right-hand side the same plot is shown but now with an input value of $\cos^2 \chi = 0.6$. The central values are shifted down to smaller values, but the absolute size of the errors stays approximately the same. This is due to the fact that most channels have large backgrounds, which are not affected by a

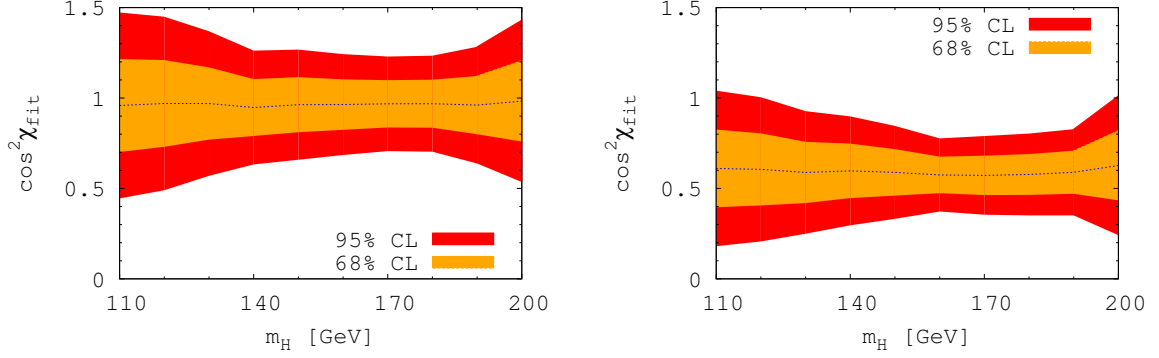


Figure 5: Precision in the Higgs portal model assuming a theory input of $\cos^2 \chi = 1$ (*left*), corresponding to the SM value, and an input value of $\cos^2 \chi = 0.6$ (*right*). Numbers assume LHC data at 14 TeV with an integrated luminosity of 30 fb^{-1} and no invisible decay modes.

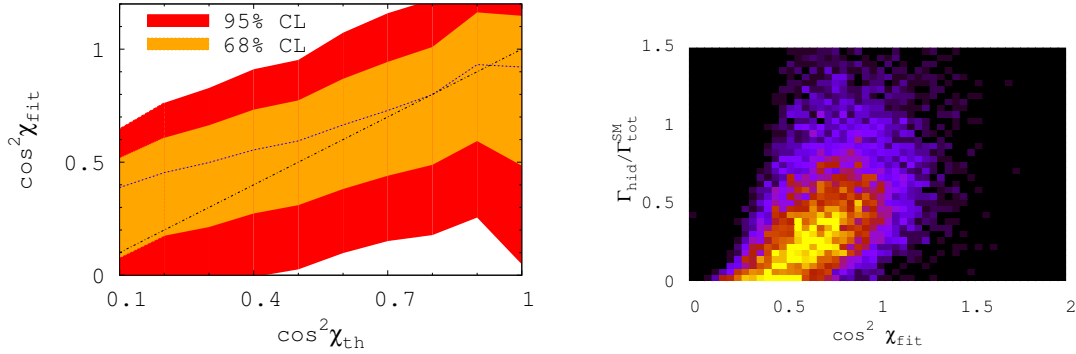


Figure 6: Precision in the Higgs portal model assuming a Higgs mass of 120 GeV and including invisible decays with $\Gamma_{\text{hid}} = \sin^2 \chi \cdot \Gamma_{\text{tot}}^{\text{SM}}$. We show the fitted value $\cos^2 \chi_{\text{fit}}$ over the input value $\cos^2 \chi_{\text{th}}$ (*left*), as well as the correlation between $\cos^2 \chi_{\text{fit}}$ and Γ_{hid} for an input value of $\cos^2 \chi_{\text{th}} = 0.6$ (*right*). Numbers assume LHC data at 14 TeV with an integrated luminosity of 30 fb^{-1} . The brightness in the correlation plot on the right-hand side denotes the resulting log-likelihood.

reduction in signal cross section. At the chosen luminosity of 30 fb^{-1} these give the dominant effect. Also, the value $\cos^2 \chi = 1$ is outside the 95% CL band over almost the whole mass range. Therefore, in this scenario the SM could be excluded at the 95% CL.

Figure 6 shows the fitted over the input $\cos^2 \chi$ for a Higgs boson mass of 120 GeV. Now decays into the invisible sector are also included with a partial width of $\sin^2 \chi$ times the SM Higgs width. This corresponds for example to the case where the hidden sector is an exact copy of the SM sector. Correspondingly, a measurement of the branching ratio into invisible particles is added [34, 35, 36]. This will be possible only with a rather low precision at the LHC. Therefore, the expected accuracy on $\cos^2 \chi$ is much lower than in the previous case, as can be seen on the left-hand side of Fig. 6. Also, at low values of $\cos^2 \chi$, we see a deviation of the fitted value, tending to be larger than the input one. This is because only measurements with a positive signal are taken into account. Positive fluctuations are hence always included, while negative ones might get removed. The observation of a Higgs signal therefore favours larger values of the coupling. On the right-hand side of Fig. 6 a correlation plot between the invisible decay width and the fitted $\cos^2 \chi$ is depicted for an input value of $\cos^2 \chi = 0.6$. A strong correlation between the two variables is visible, which is the origin of the large errors on $\cos^2 \chi$ observed before. This correlation is due to the total width of the Higgs boson, where the invisible decay width enters. As the denominator in the branching ratio it enters into all measurements.

4.2 Strongly-interacting Light Higgs

In strongly-interacting light Higgs models [20], the Higgs boson emerges as a pseudo-Goldstone boson of a new, strongly-interacting sector. As a pseudo-Goldstone boson, the Higgs can be much lighter than the other particles of the theory and therefore be in the mass range still allowed by all experimental constraints, while the other ones can be chosen heavy enough to avoid constraints from direct searches. Modifications of the Higgs-boson couplings can be parametrised by $\xi = \left(\frac{v}{f}\right)^2$, where $v = 246 \text{ GeV}$ is the SM Higgs vev and f the Goldstone scale. The limit $f \rightarrow \infty$ corresponds to the SM, while $f = v$ are Technicolour models.

There are two important phenomenological implementations. In the first one, called MCHM4, all couplings of the Higgs boson to other particles scale with $\sqrt{1-\xi}$. Therefore, the results of the Higgs portal in the previous subsection can be reused by identifying $\cos^2 \chi = 1 - \xi$ and setting invisible decay modes to zero. In the second one, MCHM5, the couplings change differently for vector bosons and fermions

$$g_{VVH} = g_{VVH}^{\text{SM}} \cdot \sqrt{1-\xi}$$

$$g_{ffH} = g_{ffH}^{\text{SM}} \cdot \frac{1-2\xi}{\sqrt{1-\xi}}.$$

The latter one has the interesting feature that the coupling vanishes for $\xi = 0.5$ and flips its sign for values below that. These models also show significant deviations in Higgs pair-production processes [37], which we will not consider further here.

In Fig. 7 we depict the fitted value of ξ over the input one for an integrated luminosity of 30 (left) and 300 fb^{-1} (right) at the 14 TeV LHC. The shaded region around $\xi = 0.5$ denotes the region where the cross sections are so low, that with the given luminosity no evidence of a Higgs boson is yet expected. For the lower luminosity there are always two possible solutions. One corresponds to the correct solution, while the other originates from the ambiguity in the fermion-Higgs coupling. The sign of the coupling is only observable as interference between W -boson and top-quark loop in the effective photon coupling. With the higher luminosity this degeneracy is lifted, as can be seen on the right-hand side of Fig. 7. This is further demonstrated in Fig. 8. Here we show the log-likelihood for 30 fb^{-1} in the two individual channels which contribute most to the parameter determination. Both channels vanish at $\xi = 0.5$ and therefore for this value the log-likelihood is constant independent of the parameter. The left channel is gluon-fusion Higgs production with decays into photons. For each input value two different solutions can be found that cannot be distinguished, as they yield the same rate. On the right-hand side, we show the combination of vector-boson associated production channels with decay into bottom quarks via subjet techniques, which are all governed by the same coupling factors. Here for $\xi \lesssim 0.4$ only a single solution exists, while for larger values additional solutions appear. These do not coincide with the secondary solution of the first channel, however,

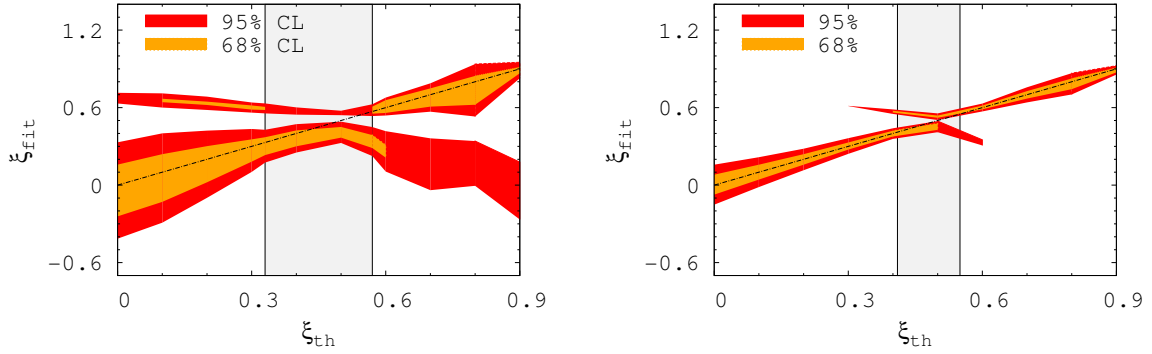


Figure 7: Best-fit values and 68% and 95% CL error bands in the MCHM5 model for the LHC at 14 TeV assuming a Higgs boson mass of 120 GeV as function of the input value ξ_{th} . Results are shown for an integrated luminosity of 30 (*left*) and 300 fb^{-1} (*right*).

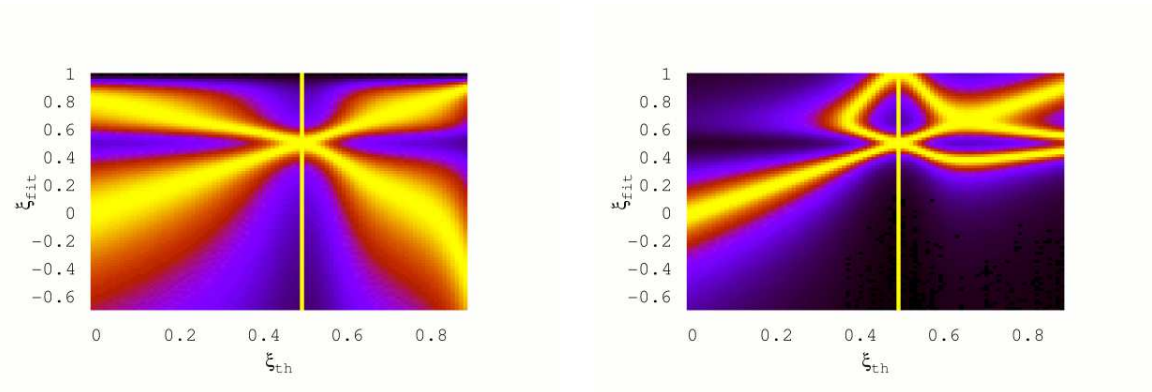


Figure 8: Best-fit distribution for two main channels: gluon-fusion production with decay into photons (*left*) and vector-boson-associated production with decay into bottom quarks (*right*). Results are shown for a Higgs boson of 120 GeV at the LHC at 14 TeV and an integrated luminosity of 30 fb^{-1} . The brightness denotes the resulting log-likelihood.

so for the nominal values the solution becomes unique. Therefore, the degeneracy is not a true one, but induced by fluctuations due to errors and can be lifted with more data.

5 Conclusions

The determination of the Higgs-boson couplings is an important task to verify our understanding of electro-weak symmetry breaking and the Higgs mechanism. We have studied how well we can measure these couplings at the LHC and what remains as a task for a future linear collider. To be independent of any specific new-physics model, we take as a model the Standard Model, where all Higgs couplings are left as free parameters. Using the SFitter framework, all experimental and theory errors, as well as their correlations, can be fully taken into account. For a single parameter modifying all couplings an error of 9% is achievable for a Higgs boson mass of 125 GeV. We have also interpreted our results in terms of new-physics models, namely a Higgs portal and a strongly-interacting light Higgs. For the former, invisible decay modes provide an additional experimental challenge. In the latter case, statistical fluctuations lead to secondary solutions, which also need to be considered.

Acknowledgments

We would like to thank the organisers of the LC-Forum for the friendly atmosphere during the workshop and the possibility to present our results. Support by the Deutsche Forschungsgemeinschaft via the Sonderforschungsbereich/Transregio SFB/TR-9 “Computational Particle Physics” and the Initiative and Networking Fund of the Helmholtz Association, contract HA-101(“Physics at the Terascale”) is acknowledged.

References

- [1] P. W. Higgs, Phys. Lett. **12**, 132 (1964); P. W. Higgs, Phys. Rev. Lett. **13**, 508 (1964); F. Englert and R. Brout, Phys. Rev. Lett. **13**, 321 (1964).
- [2] A. Djouadi, Phys. Rept. **457**, 1 (2008) [arXiv:hep-ph/0503172]. V. Büscher and K. Jakobs, Int. J. Mod. Phys. A **20**, 2523 (2005); [arXiv:hep-ph/0504099]. D. Rainwater, arXiv:hep-ph/0702124;
- [3] S. Dittmaier *et al.* [LHC Higgs Cross Section Working Group Collaboration], arXiv:1101.0593 [hep-ph]; arXiv:1201.3084 [hep-ph].
- [4] [LEP, Tevatron and SLD Collaborations and Working Groups], arXiv:0811.4682 [hep-ex].
- [5] [TEVNPH (Tevatron New Phenomina and Higgs Working Group) and CDF and D0 Collaborations], arXiv:1203.3774 [hep-ex].
- [6] ATLAS Collaboration, ATLAS-CONF-2012-019.
- [7] CMS Collaboration, CMS-PAS-HIG-12-008.
- [8] D. Y. Bardin, P. Christova, M. Jack, L. Kalinovskaya, A. Olchevski, S. Riemann and T. Riemann, Comput. Phys. Commun. **133** (2001) 229 [hep-ph/9908433]; A. B. Arbuzov, M. Awramik, M. Czakon, A. Freitas, M. W. Grunewald, K. Monig, S. Riemann and T. Riemann, Comput. Phys. Commun. **174** (2006) 728 [hep-ph/0507146].
- [9] H. Flacher, M. Goebel, J. Haller, A. Hocker, K. Monig, J. Stelzer, Eur. Phys. J. **C60**, 543-583 (2009). [arXiv:0811.0009 [hep-ph]], M. Baak, M. Goebel, J. Haller, A. Hoecker, D. Ludwig, K. Moenig, M. Schott, J. Stelzer, [arXiv:1107.0975 [hep-ph]].
- [10] D. Zeppenfeld, R. Kinnunen, A. Nikitenko and E. Richter-Was, Phys. Rev. D **62** (2000) 013009 [hep-ph/0002036]; M. Dührssen, S. Heinemeyer, H. Logan, D. Rainwater, G. Weiglein and D. Zeppenfeld, Phys. Rev. D **70**, 113009 (2004).
- [11] R. Lafaye, T. Plehn, M. Rauch, D. Zerwas and M. Dührssen, JHEP **0908**, 009 (2009) [arXiv:0904.3866 [hep-ph]], M. Rauch [SFitter Collaboration], [arXiv:1005.2843 [hep-ph]].
- [12] S. Bock, R. Lafaye, T. Plehn, M. Rauch, D. Zerwas, P. M. Zerwas, Phys. Lett. **B694**, 44-53 (2010). [arXiv:1007.2645 [hep-ph]].
- [13] F. Bonnet, M. B. Gavela, T. Ota, W. Winter, [arXiv:1105.5140 [hep-ph]].
- [14] D. Carmi, A. Falkowski, E. Kuflik and T. Volansky, arXiv:1202.3144 [hep-ph]; A. Azatov, R. Contino and J. Galloway, arXiv:1202.3415 [hep-ph]; J. R. Espinosa, C. Grojean, M. Muhlleitner and M. Trott, arXiv:1202.3697 [hep-ph]; P. P. Giardino, K. Kannike, M. Raidal and A. Strumia, arXiv:1203.4254 [hep-ph];
- [15] M. Rauch, talk at Moriond EW 2012; M. Klute, R. Lafaye, T. Plehn, M. Rauch, D. Zerwas, M. Dührssen, in preparation.

- [16] J. A. Aguilar-Saavedra *et al.* [ECFA/DESY LC Physics Working Group Collaboration], hep-ph/0106315; E. Accomando *et al.* [CLIC Physics Working Group Collaboration], hep-ph/0412251; S. Heinemeyer, S. Kanemura, H. Logan, A. Raspereza, T. M. P. Tait, H. Baer, E. L. Berger and A. Birkedal *et al.*, hep-ph/0511332; G. Aarons *et al.* [ILC Collaboration], arXiv:0709.1893 [hep-ph]; W. Lohmann, M. Ohlerich, A. Raspereza and A. Schalicke, eConf C **0705302** (2007) TIG13 [arXiv:0710.2602 [hep-ex]]; and references therein.
- [17] J. R. Dell’Aquila and C. A. Nelson, Phys. Rev. D **33**, 93 (1986).; D. J. Miller, 2, S. Y. Choi, B. Eberle, M. M. Muhlleitner and P. M. Zerwas, Phys. Lett. B **505** (2001) 149 [hep-ph/0102023]; T. Plehn, D. Rainwater and D. Zeppenfeld, Phys. Rev. Lett. **88**, 051801 (2002); C. P. Buszello, I. Fleck, P. Marquard and J. J. van der Bij, Eur. Phys. J. C **32**, 209 (2004); V. Hankele, G. Klamke, D. Zeppenfeld and T. Figy, Phys. Rev. D **74**, 095001 (2006); C. Ruwiedel, N. Wermes and M. Schumacher, Eur. Phys. J. C **51**, 385 (2007); K. Hagiwara, Q. Li and K. Mawatari, JHEP **0907** (2009) 101 [arXiv:0905.4314 [hep-ph]]; C. Englert, C. Hackstein and M. Spannowsky, Phys. Rev. D **82** (2010) 114024 [arXiv:1010.0676 [hep-ph]]; R. M. Godbole, C. Hangst, M. Muhlleitner, S. D. Rindani and P. Sharma, Eur. Phys. J. C **71** (2011) 1681 [arXiv:1103.5404 [hep-ph]]; J. Ellis and D. S. Hwang, arXiv:1202.6660 [hep-ph]; C. Englert, M. Spannowsky and M. Takeuchi, arXiv:1203.5788 [hep-ph]; M. Muhlleitner, these proceedings.
- [18] for an introduction see e.g. S. P. Martin, arXiv:hep-ph/9709356; I. J. R. Aitchison, arXiv:hep-ph/0505105; J. F. Gunion and H. E. Haber, Phys. Rev. D **67**, 075019 (2003).
- [19] T. Binoth and J. J. van der Bij, Z. Phys. C **75**, 17 (1997); A. Hill and J. J. van der Bij, Phys. Rev. D **36** (1987) 3463; R. Schabinger and J. D. Wells, Phys. Rev. D **72**, 093007 (2005); B. Patt, F. Wilczek, [hep-ph/0605188]; C. Englert, T. Plehn, D. Zerwas and P. M. Zerwas, Phys. Lett. B **703** (2011) 298; C. Englert, T. Plehn, M. Rauch, D. Zerwas and P. M. Zerwas, Phys. Lett. B **707** (2012) 512 [arXiv:1112.3007 [hep-ph]]; B. Batell, S. Gori and L. -T. Wang, arXiv:1112.5180 [hep-ph]; A. Djouadi, O. Lebedev, Y. Mambrini and J. Quevillon, Phys. Lett. B **709** (2012) 65 [arXiv:1112.3299 [hep-ph]]; C. Englert, these proceedings.
- [20] G. F. Giudice, C. Grojean, A. Pomarol, R. Rattazzi, JHEP **0706**, 045 (2007). [hep-ph/0703164], J. R. Espinosa, C. Grojean and M. Muhlleitner, JHEP **1005**, 065 (2010) arXiv:1003.3251 [hep-ph]; J. R. Espinosa, C. Grojean and M. Muhlleitner, arXiv:1202.1286 [hep-ph].
- [21] A. Höcker, H. Lacker, S. Laplace and F. Le Diberder, Eur. Phys. J. C **21**, 225 (2001); J. Charles *et al.* arXiv:hep-ph/0607246.
- [22] R. Lafaye, T. Plehn, M. Rauch and D. Zerwas, Eur. Phys. J. C **54**, 617 (2008).
- [23] A. Djouadi, J. Kalinowski and M. Spira, Comput. Phys. Commun. **108** (1998) 56 [hep-ph/9704448]; A. Djouadi, M. M. Muhlleitner and M. Spira, Acta Phys. Polon. B **38** (2007) 635 [hep-ph/0609292].
- [24] T. Plehn and D. Rainwater, Phys. Lett. B **520**, 108 (2001); K. Cranmer and T. Plehn, Eur. Phys. J. C **51**, 415 (2007); see also T. Han and B. McElrath, Phys. Lett. B **528**, 81 (2002).
- [25] S. Su and B. Thomas, arXiv:0812.1798 [hep-ph].
- [26] U. Baur, T. Plehn and D. L. Rainwater, Phys. Rev. Lett. **89**, 151801 (2002) and Phys. Rev. D **67**, 033003 (2003); A. Dahlhoff, arXiv:hep-ex/0505022; for a different point of view see also F. Gianotti *et al.*, arXiv:hep-ph/0204087.
- [27] V. Barger, T. Han, P. Langacker, B. McElrath and P. Zerwas, Phys. Rev. D **67**, 115001 (2003); C. Grojean, G. Servant and J. D. Wells, Phys. Rev. D **71**, 036001 (2005); S. Kanemura, Y. Okada, E. Senaha and C. P. Yuan, Phys. Rev. D **70**, 115002 (2004).
- [28] T. Plehn and M. Rauch, Phys. Rev. D **72**, 053008 (2005); T. Binoth, S. Karg, N. Kauer and R. Rückl, Phys. Rev. D **74**, 113008 (2006).
- [29] F. Boudjema and E. Chopin, Z. Phys. C **73** (1996) 85 [hep-ph/9507396]; A. Djouadi, W. Kilian, M. Muhlleitner and P. M. Zerwas, Eur. Phys. J. C **10** (1999) 27 [hep-ph/9903229]; J. Tian, K. Fujii and Y. Gao, arXiv:1008.0921 [hep-ex].
- [30] M. Dürrssen, ATL-PHYS-2003-030.
- [31] M. Rauch, arXiv:1110.1196 [hep-ph].
- [32] T. Gleisberg, S. Hoeche, F. Krauss, M. Schonherr, S. Schumann, F. Siegert and J. Winter, JHEP **0902** (2009) 007 [arXiv:0811.4622 [hep-ph]].
- [33] J. M. Butterworth, A. R. Davison, M. Rubin and G. P. Salam, Phys. Rev. Lett. **100**, 242001 (2008), ATLAS Collaboration, ATL-PHYS-PUB-2009-088.
- [34] O. J. Éboli and D. Zeppenfeld, Phys. Lett. B **495**, 147 (2000).
- [35] G. Aad *et al.* [The ATLAS Collaboration], arXiv:0901.0512 [hep-ex].
- [36] G. L. Bayatian *et al.* [CMS Collaboration], J. Phys. G **34**, 995 (2007).
- [37] R. Gröber, M. Muhlleitner, JHEP **1106**, 020 (2011) [arXiv:1012.1562 [hep-ph]]; R. Gröber, LC-TH-2012-001.